Synthesis and Cytotoxicity Evaluation of Novel Andrographolide-1,2,3-Triazole Derivatives

Yakaiah Chinthala,[a] Manjulatha K,[b] Pooja Sharma,[c] Satya Srinivas KVN,[a] Kotesh Jonnala,[a]* Niranjana Kumar Arigari,[a] Feroz Khan,[c] and Setty OH[b]

[a]Natural Product Chemistry, CSIR-Central Institute of Medicinal and Aromatic Plants-Research Centre, Boduppal, Hyderabad 500092, Telangana, India
[b]Department of Biochemistry, School of Life Sciences, University of Hyderabad, India
[c]Metabolic and Structural Biology Department, CSIR-Central Institute of Medicinal and Aromatic Plants Kukrail Picnic Spot Road, Lucknow 226015, Uttar Pradesh, India
*E-mail: koteshkumarj@yahoo.com

Additional Supporting Information may be found in the online version of this article.
Received March 19, 2015
DOI 10.1002/jhet.2505
Published online 00 Month 2015 in Wiley Online Library (wileyonlinelibrary.com).

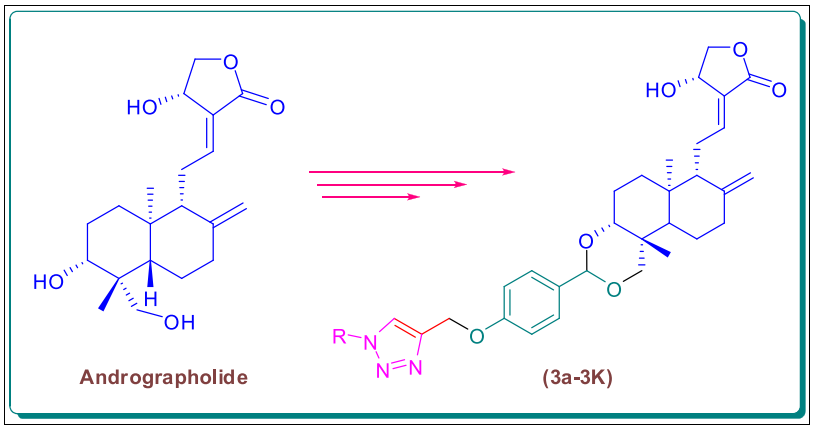

A series of new andrographolide-1,2,3-triazole derivatives, **3a–k**, were synthesized from a natural bioactive labdane type diterpenoid, andrographolide. All the derivatives were screened against human cancer cell lines MCF7, MDA-MB-231, COLO205, HepG2, K562, Hela, and HEK293 to evaluate their cytotoxic activity. All the compounds showed anticancer activity selectively against K562 cell line, with IC_{50} values ranging from 8.00 to 17.11 μ*M*, and are inactive against the rest of the cell lines. Compounds **3c** and **3d** showed significant cytotoxicity among the synthesized derivatives. The *in silico* docking studies revealed compounds **3b** and **3d** with high binding affinity against the cancer target, transient receptor potential vanilloid 1.

INTRODUCTION

Andrographis paniculata, a common herb of medicines, is widely distributed in China, India, and other Asian countries [1,2]. The extracts of this species exhibit various biological activities such as hepatoprotective [3], antibacterial [4], anti-inflammatory [5,6], antidiabetic [7], anticancer [8,9] and so on. Labdane diterpenoids such as deoxyandrographolide and andrographolide (Fig. 1) are the principal active constituents of this plant. In recent past, the structure–activity relationship studies of analogues of andrographolides as active anticancer [10–12] and anti-inflammatory agents [13] were influenced to design diversified analogues with the better bioactivity and water solubility properties. Thus, there is a need to prepare new andrographolide derivatives with structural diversity by introducing lead heterocyclic pharmacophores such as 1,2,3-triazoles. The 1,2,3-triazoles have received much attention because of its wider range of applications as agrochemicals, pharmaceuticals, dyestuffs, antimicrobial [14,15], cytostatic, virostatic [16], antimalarial [17], and anti-inflammatory activities [18]. Thus, it is interesting to look into the bioactivity profiles of molecules made of andrographolide with substituted 1,2,3-triazoles. The present investigation is aimed at synthesizing *N*-aryl-substituted 1,2,3-triazoles attached to andrographolide moiety via a methylene bridge by a protocol as shown in Scheme 1 and evaluating the resulting derivatives for their cytotoxic activity.

RESULTS AND DISCUSSION

Chemistry. The synthetic strategy followed for the synthesis of different andrographolide triazoles is outlined in Scheme 1. A series of compounds **3a–k** were synthesized in three steps. In the first step, 4-hydroxybenzaldehyde was reacted with propargyl bromide in the presence of potassium carbonate at reflux condition to obtain compound **1a**. In the second step, andrographolide was condensed with 4-(prop-2-ynyloxy)

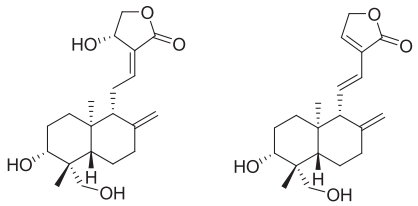

Andrographolide 14-deoxy-11,12-didehydro andrographolide

Figure 1. Structures of compounds isolated from *Andrographis paniculata*.

benzaldehyde (**1a**) in the basic medium to give respective **2b**. In the final step, the **2b** was further reacted with appropriately substituted aromatic azides by a click reaction to afford compounds **3a–k**. All the synthesized compounds were characterized by spectroscopy such as IR, ^{1}H, and ^{13}C NMR and mass. In the ^{1}H NMR, the presence of singlet resonances from δ 5.2–5.9 ppm was due to methylene bridge protons in compounds **3a–k**. In the IR spectra, the aliphatic C–H stretching of methylene group in compounds **3a–k** appeared at 2900–2960 cm^{-1}, while the aromatic C–H stretching frequencies were observed in between 3000 and 3130 cm^{-1}. Spectral data for all the new compounds were presented in Experimental section.

Pharmacological screening. ***Anticancer activity.*** The synthesized triazole derivatives of andrographolide **3a–k** were evaluated by MTT assay against seven human cancer cell lines, MCF7 (creast), MDA-MB-231 (breast), COLO205 (colorectal), HepG2 (hepato), K562 (myelogenous leukemia), HeLa (cervical) and HEK293 (normal human kidney embryonic). In general, the leukemic cell lines were more sensitive to the derivatives with IC_{50} values ranging from 8.00 to 17.11 μ*M*, and the rest of the cell lines MCF7, MDA-MB-231, COLO205, HepG2, and HeLa were found to be inactive. Compounds **3c** and **3d** were shown better

Scheme 1. Synthesis of andrographolide 1,2,3-triazole derivatives.

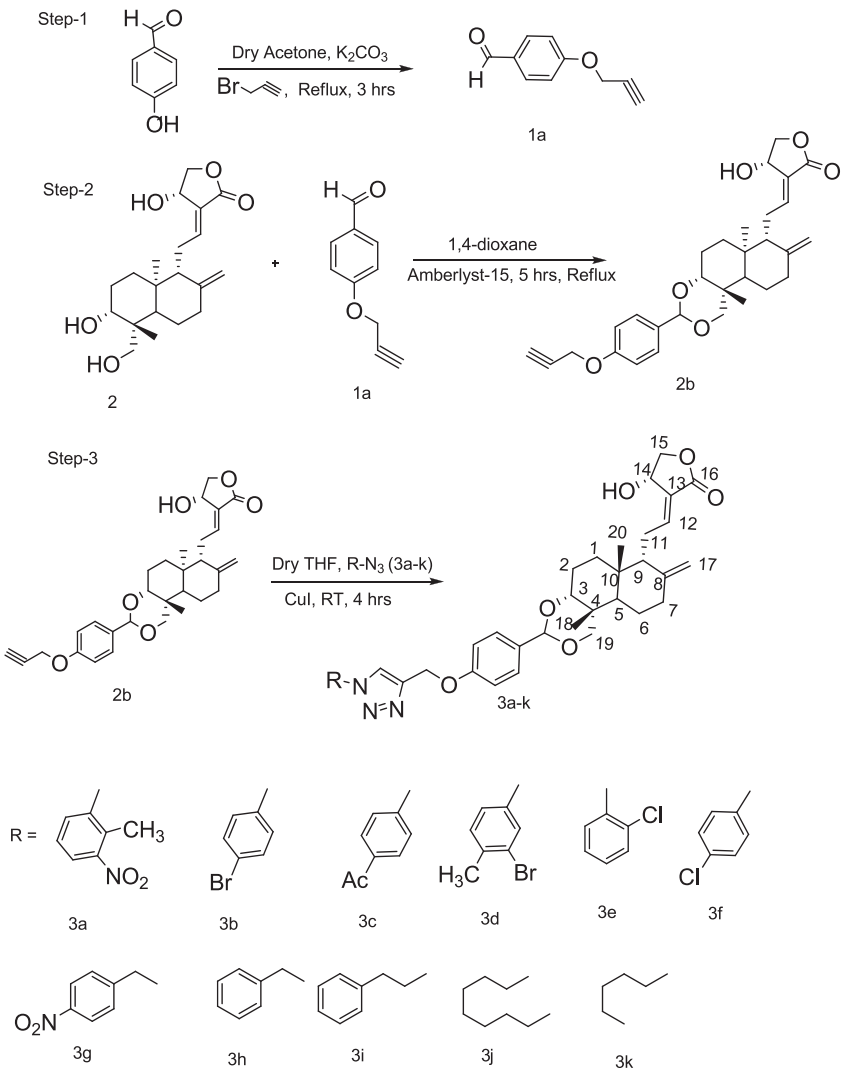

Table 1

Anticancer activity results of synthesized derivatives **3a–k**.

Compound	K562 cancer cell line			HEK cell line	
	Inhibition at 50 μ*M*			Inhibition at 100 μ*M*	
	Mean	SD	IC_{50} (μ*M*)	Mean	SD
3a	46.33	±1.90	10.69	−8.09	±1.122
3b	31.13	±4.97	15.90	−13.87	±1.241
3c	62.95	±1.95	8.00	−14.25	±1.162
3d	51.86	±2.48	9.72	−20.44	±1.910
3e	41.51	±1.13	12.17	−15.56	±1.403
3f	43.87	±1.09	11.37	−15.71	±1.186
3g	42.94	±2.23	11.66	1.77	±0.679
3h	29.26	±0.97	17.11	−17.50	±0.977
3i	31.75	±1.73	15.65	−3.23	±0.753
3j	42.81	±0.84	11.37	−1.04	±0.481
3k	41.33	±0.47	12.10	−12.49	±1.365
Doxorubicin	95.58	±1.97	0.09	91.89	±0.145

SD, standard deviation

cytotoxicity towards K562 cell lines when compared with the other compounds in the series with 62.9% and 51.8% inhibition at 50-μ*M* concentration with IC_{50} values of 8 and 9.7 μ*M*, respectively (Table 1). The order of inhibition found as **3c** > **3d** > **3b** > **3f** > **3g** > **3j** > **3e** > **3k** > **3i** > **3a** > **3h** at 50-μ*M* concentration and with IC_{50} values ranged from 10.6 to 17.1 μ*M*. Andrographolide-1,2,3-triazole can be considered as parent moiety, and the substitution at the first position of triazole was varied. It is very clear that the first position with a substituted benzene ring (**3c**, **3d**, **3a**, **3f**, **3g**) found to be active over unsubstituted (**3i**, **3h**) or aliphatic (**3j**, **3k**, **3h**) substitution, and electron-donating groups (**3c**, **3d**, **3f**) are preferred over withdrawing (**3g**) groups. The increase in the carbon chain length linking the substituted benzene with the triazole group reduces the activity (**3h** and **3i**). The results clearly indicated that these analogues were non-toxic and had no inhibitory effect on cell proliferation in HEK-293 (normal cell line) and there was minimal reduction in cell survivability. The percentage viability was above 95% at the highest concentration of 100 μ*M*.

Molecular docking studies. The objective of docking studies was to explore the binding affinity of studied compounds against selected target transient receptor potential vanilloid 1 (TRPV1, Figure S1, in Supplementary Information). To identify the molecular target, a more comprehensive functional pathway database MetaDrug has been used. From MetaDrug, six targets named TRPV2, TRPV4, TRPV6, epithelial calcium channel, capsaicin receptor (TRPV1) and TRPV3 were identified. Endogenous expression of TRPV5 and TRPV6 calcium channels is already reported in human leukemia K562 cells [19]. Besides this, it is also reported that TRPV1 antagonist sensitizes colorectal cancer cells to apoptosis by TNF-related apoptosis-inducing ligand (TRAIL) through ROSg–JNK–CHOP-mediated upregulation of death receptors [20]. It is also reported that some of the TRPV1 antagonists cause a significant decrease of cell growth rate in human breast cancer cell line MCF-7 [21]. Considering these references, TRPV1 have been selected to explore the possible mechanism of binding residues and also because of its co-crystallized ligand, that is, capsaicin, which has been considered as positive control during docking studies. Three-dimensional crystal structure of constitutive TRPV1 (Protein Data Bank: 3J5R) were retrieved from repository of experimental explicated crystal structure of biological macromolecules available in the Protein Data Bank database (Brookhaven, NY, USA). Compound **3d** showed maximum binding affinity ($-9.4\,kcal\,mol^{-1}$) towards the target (Table 2 and Fig. 2). The binding pocket residues are mostly hydrophobic in nature. This molecular docking result indicates that the selected analogues are showing strong stability inside the TRPV1 active site. The conserved binding site amino acid residues within a selection radius of 4 Å from bound ligand **3d** were basic (polar, hydrophobic, and positive charged), for example, lysine (LYS-571), arginine (ARG-409 and ARG-557), and nucleophilic (polar and hydrophobic), for example, serine (SER-404, SER-510, and SER-512) and aliphatic, for example, valine (VAL-508 and VAL-567) and aromatic (hydrophobic), for example, tyrosine (TYR-511) and hydrophobic, for example, isoleucine (ILE-696 and ILE-703), leucine (LEU-574 and LEU-699), and acidic (polar and negative charged), for example, glutamic acid (GLU-513 and GLU-570), aspartic acid (ASP-509), and polar amide, for example, glutamine (GLN-700) with two H-bonds of length 2.4 (SER-404) and 2.0 (SER-512). Most of

Table 2

Docking results of active compounds.

Sample	Binding energy (kcal/mol)	Amino acid residues (within a radius of 4 Å)	H-bond formation
Capsaicin	−6.0	SER-402,SER-403,SER-404,ARG-409,VAL-508,ASP-509,SER-510, TYR-511,SER-512,GLU-513,ARG-557,VAL-567,GLU-570,LYS-571, LEU-574,ILE-696,LEU-699,GLN-700,ILE-703	2.3, 2.8 (ARG-557)
3a	−7.9	SER-404,ARG-409,VAL-508,ASP-509,SER-510,TYR-511,SER-512, GLU-513,ARG-557,VAL-567,GLU-570,LYS-571,LEU-574,ILE-696, LEU-699,GLN-700,ILE-703	2.8, 2.4 (SER-404) 2.0 (SER-512)
3b	−9.3	SER-404,ARG-409,VAL-508,ASP-509,SER-510,TYR-511,SER-512, GLU-513,ARG-557,VAL-567,GLU-570,LYS-571,LEU-574,ILE-696, LEU-699,GLN-700,ILE-703	2.1 (SER-512) 2.2 (SER-404)
3c	−9.1	SER-404,ARG-409,VAL-508,ASP-509,SER-510,TYR-511,SER-512, GLU-513,ARG-557,VAL-567,GLU-570,LYS-571,LEU-574,ILE-696, LEU-699,GLN-700,ILE-703	2.3 (ARG-409) 2.6 (SER-403) 2.7 (SER-510) 2.8 (GLU-513) 2.2 (VAL-508)
3d	−9.4	SER-404,ARG-409,VAL-508,ASP-509,SER-510,TYR-511,SER-512, GLU-513,ARG-557,VAL-567,GLU-570,LYS-571,LEU-574,ILE-696, LEU-699,GLN-700,ILE-703	2.4 (SER-404) 2.0 (SER-512)
3e	−9.2	SER-404,ARG-409,VAL-508,ASP-509,SER-510,TYR-511,SER-512, GLU-513,ARG-557,VAL-567,GLU-570,LYS-571,LEU-574,ILE-696, LEU-699,GLN-700,ILE-703	2.2 (SER-512) 2.2 (ARG-409)
3f	−9.3	SER-404,ARG-409,VAL-508,ASP-509,SER-510,TYR-511,SER-512, GLU-513,ARG-557,VAL-567,GLU-570,LYS-571,LEU-574,ILE-696, LEU-699,GLN-700,ILE-703	2.1 (SER-512) 2.2 (ARG-409)
3g	−9.1	SER-404,ARG-409,VAL-508,ASP-509,SER-510,TYR-511,SER-512, GLU-513,ARG-557,VAL-567,GLU-570,LYS-571,LEU-574,ILE-696, LEU-699,GLN-700,ILE-703	2.5, 2.3 (ARG-409) 2.1 (SER-512)
3h	−8.3	SER-404,ARG-409,VAL-508,ASP-509,SER-510,TYR-511,SER-512, GLU-513,ARG-557,VAL-567,GLU-570,LYS-571,LEU-574,ILE-696, LEU-699,GLN-700,ILE-703	2.6 (ARG-409) 2.5 (SER-404) 2.4 (VAL-508) 2.6, 2.0 (ARG-557)
3i	−7.8	SER-404,ARG-409,VAL-508,ASP-509,SER-510,TYR-511,SER-512, GLU-513,ARG-557,VAL-567,GLU-570,LYS-571,LEU-574,ILE-696, LEU-699,GLN-700,ILE-703	2.6 (SER-510) 2.8 (GLU-513)
3j	−7.7	SER-404,ARG-409,VAL-508,ASP-509,SER-510,TYR-511,SER-512, GLU-513,ARG-557,VAL-567,GLU-570,LYS-571,LEU-574,ILE-696, LEU-699,GLN-700,ILE-703	2.5 (SER-510) 2.8 (GLU-513) 2.5 (SER-404) 2.3 (ARG-409)
3k	−8.4	SER-404,ARG-409,VAL-508,ASP-509,SER-510,TYR-511,SER-512, GLU-513,ARG-557,VAL-567,GLU-570,LYS-571,LEU-574,ILE-696, LEU-699,GLN-700,ILE-703	2.3 (SER-409) 2.6 (SER-510) 2.8 (SER-512)

the drug failures at early pipeline occur because of undesirable pharmacokinetics and toxicity problems. The pharmacokinetic properties were calculated to check the compliance of all compounds with standard descriptors. Aqueous solubility, blood brain barrier penetration, cytochrome P450 2D6 binding, hepatotoxicity, intestinal absorption, and plasma protein binding were evaluated and summarized in Table S1 (in Supplementary Information) together with a biplot in Figure 3. The biplot showed the two analogous 95% and 99% confidence ellipses for the blood brain barrier penetration and human intestinal absorption models, respectively. The model was developed using synthesized derivatives based on the calculations AlogP (ADMET_AlogP98) and 2D polar surface area. Table S1 (in Supplementary Information) shows that all compounds have low aqueous solubility, undefined blood brain barrier penetration level, and hepatotoxicity level of 0 (non-toxic) with the exception of compound capsaicin, which is a control drug. Non-inhibitors of cytochrome P450 2D6 (CYP2D6), which indicates that all compounds may be well metabolized in phase I metabolism. All compounds are highly (≥90%) bound to carrier proteins in the blood. Here, the acyclic diene metathesis (ADMET) predicted result shows that all the compounds cannot be easily absorbed by the intestine in comparison with capsaicin (good absorption) and **3a** (moderate absorption). Although the drug-likeness parameter results showed that all compounds violate Lipinski's rule of five but within acceptable limit, in comparison with capsaicin (Table S2, in Supplementary Information). Computational toxicity parameters were calculated for all the compounds through Discovery

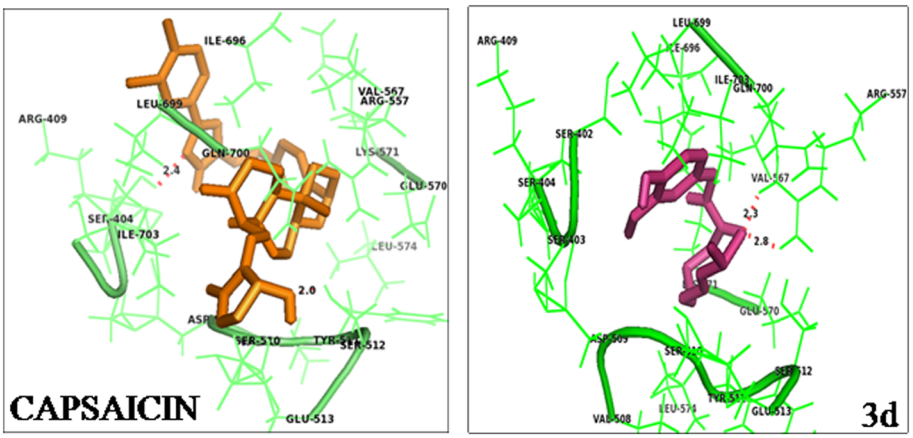

Figure 2. Docking results of studied compound on anticancer cell line K562. (i) Docked control drug capsaicin on TRPV1 with docking energy of −6.0 kcal/mol, and (ii) docked compound **3d** on TRPV1 with high docking energy −9.4 kcal/mol. [Color figure can be viewed in the online issue, which is available at wileyonlinelibrary.com.]

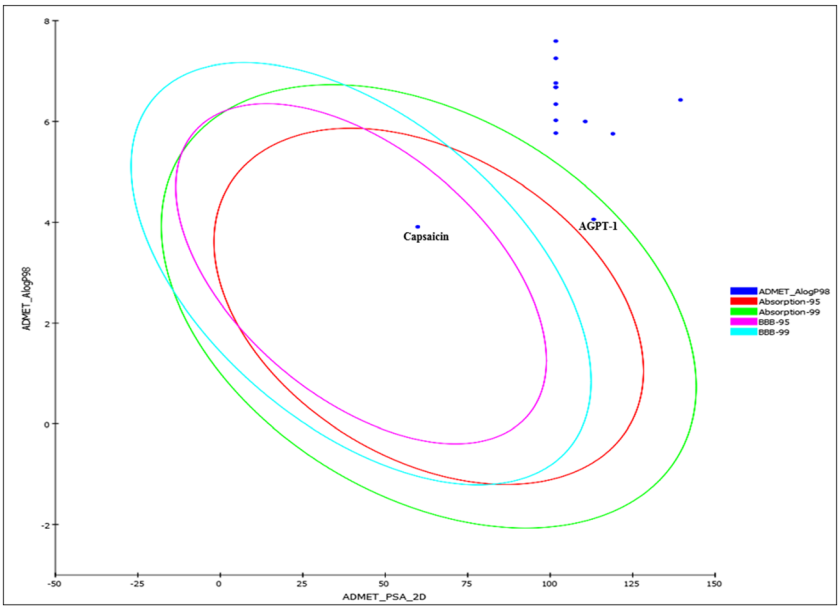

Figure 3. Prediction of drug absorption for various polar surface area (PSA) considered for anti-malarial activity. [Color figure can be viewed in the online issue, which is available at wileyonlinelibrary.com.]

Studio v3.5 (Accelrys, San Diego, CA). TOPKAT in Accelrys predicts toxicity endpoints based on chemical structure, including Ames mutagenicity, rat oral LD_{50}, developmental toxicity prediction, skin irritation, National Toxicology Program (NTP) prediction, and mouse male/female Food and Drug Administration (FDA) prediction. Various models that can be calculated are tabulated in Table S3 (in Supplementary Information). From the computed probability and toxicity analysis, all compounds have proven to be non-mutagenic, with skin irritancy. Compounds **3b**, **3a**, **3d**, **3g**, and **3k** showed carcinogenicity to NTP prediction, and compound **3b** is more toxic than all other compounds.

The ADME 2-D graph for each compound was plotted against AlogP98 versus PSA_2D (polar surface area). The area encompassed by the ellipse is a prediction of good absorption with no violation of ADMET properties. On the basis of the absorption model of Egan *et al.* [22] the 95% and 99% confidence limit ellipses corresponding to the blood brain barrier and intestinal absorption models are indicated.

CONCLUSION

New andrographolide derivatives **3a–k** were prepared by applying an efficient click chemistry strategy and

screened for anticancer activity against different human cancer cell lines. These compounds showed cytotoxicity selectively towards K562 cell lines and were inactive to the rest of the cell lines. Introduction of substituted aromatic ring along with 1,2,3-triazole in the andrographolide skeleton enhanced their activity selectively against leukemic cell lines and is also non-toxic to normal human cell lines. The docking studies of andrographolide derivatives showed that compounds **3d** and **3b** possess high binding affinity against one of the potential cancer targets, TRPV1. The docking studies of active andrographolide-1,2,3-triazole (AGPT) derivatives showed that compound **3d** and **3a** possess high binding affinity against TRPV1. The molecular docking results of active AGPT derivatives showed that the main residues in the active binding site pocket of TRPV1 are hydrophobic in nature. Main influencing factors of molecular interactions between TRPV1 and AGPT derivatives were H-bond, hydrophobic, and electrostatic interactions. The calculated parameters of the studied AGPT derivatives for drug likeness (Lipinski's rule of five), pharmacokinetic (PK) (absorption, distribution, metabolism, excretion (ADME)), and toxicity risk assessment were within the acceptable limit.

EXPERIMENTAL

Chemistry. Melting points of all the compounds were recorded on Casia-Siamia (VMP-AM) (Mumbai, India) melting point apparatus and were uncorrected. IR spectra were recorded on a PerkinElmer FTIR 240-C spectrometer (Waltham, MA, USA) using KBr pellets. NMR spectra were recorded on Bruker Avance 300 MHz (Billerica, MA, USA) in $CDCl_3$ and dimethyl sulfoxide (DMSO)-d_6 using TMS as the internal standard. Electron impact and chemical ionization mass spectra were recorded on a VG Micro mass model 7070H instrument (Colorado, USA). All the reactions were monitored on silica gel percolated thin-layer chromatography plates of Merck (Kenilworth, NJ, USA), and spots were visualized with UV light. Silica gel (100–200 mesh) used for column chromatography was procured from Merck.

General procedure for synthesis of andrographolide derivatives 3a–k procedure for propargylation for synthesis of 4-(prop-2-ynyloxy) benzaldehyde (1a). 4-hydroxy benzaldehyde (1.0 mol) along with 1.5 mol of potassium carbonate was taken in dimethylformamide and added to this solution of propargyl bromide (1.5 mol) in dimethylformamide. Reaction mixture was stirred (reflux) to afford crude 4-(prop-2-ynyloxy) benzaldehyde. This crude compound was column chromatographed over silica gel (100–200 mesh) and eluted with 15% ethyl acetate in *n*-hexane to obtain pure compound (**1a**). White solid, yield 92%, mp 76–78°C; ^{1}H NMR ($CDCl_3$, 300 MHz): δ 2.57 (s, 1H, acetylene-H), 4.29–4.79 (s, 2H, CH_2), 7.09–7.11 (d, 2H, Ar), 7.86–7.88 (d, 2H, Ar), 9.99 (s, 1H, CHO).

General procedure for synthesis of 3-(2-(6a,10b-dimethyl-8-methylene-3-(4-(prop-2-ynyloxy)phenyl)decahydro-1H-naphtho[2,1-d][1,3]dioxin-7-yl)ethylidene)-4-hydroxydihydrofuran-2(3H)-one (2b). A mixture of andrographolide (100 mg, 0.285 mmol), 4-(prop-2-ynyloxy) benzaldehyde (**2b**) (0.855 mmol), and activated Amberlyst-15 (10 mg) in dry 1,4-dioxane (4 mL) was refluxed for 5 h under N_2 atmosphere. The reaction mixture was cooled and filtered to remove the catalyst. The organic layer was evaporated in vacuum, and the residue was subjected to the column chromatography on silica gel, and elution with petroleum ether (60–80°C)/ethyl acetate (80:20) gave **2b**. Pale yellow solid, yield 95 mg (74%), mp 176–177°C; IR ($CHCl_3$): 3397, 2962, 1738, 1216, 1097, 756 cm^{-1}; ^{1}H NMR ($CDCl_3$, 300 MHz): δ 0.89 (s, 3H, H-20), 1.22–1.32 (m, 4H, overlapped signal), 1.50 (s, 3H, H-18), 1.79–1.94 (m, 4H), 2.01–2.1 (m, 1H), 2.42–2.52 (m, 3H), 2.56–2.61 (m, 2H), 3.57–3.61 (d, 1H, J = 11.5 Hz), 3.7–3.71 (dd, 1H, J = 4.5, 4.7 Hz), 4.21–4.29 (m, 2H), 4.42–4.48 (m, 1H), 4.65 (s, 1H), 4.70–4.71 (d, 2H, J = 2.4 Hz, H-15), 4.94 (s, 1H), 5.00–5.01 (bs, 1H, H-14), 5.75 (s, 1H), 6.95–7.00 (m, 3H, Ar), 7.45–7.47 (d, 2H, J = 8.7 Hz, Ar); ^{13}C NMR (75 MHz, $CDCl_3$): δ 15.8 (CH_3, C-20), 22.2 (CH_2, C-6), 23.2 (CH_3, C-18), 25.2 (CH_2, C-11), 25.2 (CH_2, C-2), 26.5 (CH_2, C-1), 36.5 (CH_2, C-7), 37.3 (C, C-10), 38.0 (C, C-4), 39.3 (CH, C-9), 55.2 (CH, C-5), 56.2 (CH_2, C-19), 56.3 (CH_2-O), 66.5 (CH, C-14), 69.8 (CH_2, C-15), 75.9 (acetylene-C), 78.9 (acetylene-C), 81.1 (CH, C-3), 95.3 (Ar-CO), 109.6 (CH_2, C-17), 115.2 (Ar-C), 127.9 (Ar-C), 128.4 (Ar-C), 132.7 (C, C-13), 146.9 (C, C-8), 149.2 (CH, C-12), 158.3 (Ar-O), 170.5 (C, C-16); ESI-MS: m/z: 493 (M^+ 1) observed for $C_{30}H_{36}O_6$.

Synthesis of andrographolide 1,2,3-triazole derivatives (3a–k). Intermediate **2b** (1.0 mmol) was dissolved in dry tetrahydrofuran (10 mL), and catalytic amount of copper iodide was added. To this, substituted aromatic azides (1.0 mmol) in dry tetrahydrofuran were added slowly while stirring at room temperature under nitrogen atmosphere for 12 h. Later, the solvent was removed under reduced pressure, and the residue was diluted with distilled water and extracted thrice with dichloromethane. The combined organic layers were dried over anhydrous Na_2SO_4 and concentrated to acquire the product. The crude product was purified by column chromatography with ethyl acetate in hexane.

3-(2-(6a,10b-dimethyl-3-(4-((1-(2-methyl-3-nitrophenyl)-1H-1,2,3-triazol-4-yl)methoxy)phenyl)-8-methylenedecahydro-1H-naphtho[2,1-d][1,3]dioxin-7-yl)ethylidene)-4-hydroxydihydrofuran-2(3H)-one (3a). Yellow solid, yield 89%, mp 120–122°C; IR (KBr): 3279 (C–H), 3058 (Ar–H), 2922 (C–H), 2112 (C≡C), 1584 (C=N), 1466, 757 (C–N) cm^{-1}; ^{1}H NMR ($CDCl_3$, 300 MHz): δ 0.82 (s, 3H, H-20), 1.18–1.25 (m, 4H), 1.43 (s, 3H, H-18), 1.72–1.87 (m, 4H), 1.99–2.03 (d, 2H, J = 12.25 Hz), 2.23 (s, 3H, Ar-CH_3), 2.35–2.42

(2H, m), 2.50–2.55 (m, 2H), 3.51–3.55 (d, 1H, J = 11.11 Hz), 3.58–3.64 (dd, 1H, J = 4.52, 5.3 Hz), 4.18–4.22 (d, 2H, J = 11 Hz), 4.37–4.43 (m, 1H), 4.58 (s, 1H, H-17), 4.86 (s, 1H, H-17), 4.97–4.99 (d, 1H, J = 5.1 Hz), 5.28 (s, 2H, CH_2-O), 5.68 (s, 1H, Ar-CH), 6.89–6.97 (m, 2H, Ar), 7.38–7.40 (d, 2H, J = 8.5 Hz, Ar), 7.44–7.5 (m, 1H, Ar), 7.54–7.57 (d, 1H, J = 7.7 Hz, Ar), 7.70 (s, 1H, triazole-H), 7.97–7.99 (d, 1H, J = 7.9 Hz, Ar); ^{13}C NMR (75 MHz, $CDCl_3$): δ 14.9 (CH_3, Ar), 15.7 (CH_3, C-20), 22.2 (CH_2, C-6), 23.2 (CH_2, C-18), 25.2 (CH_2, C-11), 26.4 (CH_2, C-2), 36.5 (CH_2, C-1), 37.3 (CH_2, C-7), 37.9 (C, C-10), 39.3 (C, C-4), 55.3 (CH, C-9), 56.4 (CH, C-5), 62.4 (CH_2, C-19), 66.6 (CH, C-14), 70.0 (CH_2, C-15), 74.7 (CH_2-O), 81.1 (CH, C-3), 95.3 (Ar-CO), 109.6 (CH_2, C-17), 115.1 (CH, Ar), 125.0 (CH, Ar), 126.2 (CH, Ar), 127.7 (CH, Ar), 128.1 (CH, Ar), 128.5 (CH, Ar), 129.3 (CH, Ar), 130.1 (CH, Ar), 131.0 (C, C-13), 132.8 (C, Ar), 138.5 (C, Ar), 145.2, 146.9 (C, C-8), 149.1 (CH, C-12), 158.8 (Ar-NO2), 176.5 (C, C-16); ESI-MS: m/z 671 (M^+ 1) observed for $C_{37}H_{42}N_4O_8$.

3-(2-(3-(4-((1-(4-bromophenyl)-1H-1,2,3-triazol-4-yl)methoxy) phenyl)-6a,10b-dimethyl-8-methylenedecahydro-1H-naphtho [2,1-d][1,3]dioxin-7-yl)ethylidene)-4-hydroxydihydrofuran-2 (3H)-one (3b). Yellow solid, yield 93%, mp 205–206°C; IR (KBr): 3279 (C–H), 3058 (Ar–H), 2922 (C–H), 2112 (C≡C), 1584 (C=N), 1466, 757 (C–N) cm^{-1}; ^{1}H NMR ($CDCl_3$, 300 MHz): δ 0.99 (s, 3H, H-20), 1.28–1.50 (m, 4H), 1.53 (s, 3H, H-18), 1.71–1.80 (bs, 2H), 1.90–2.09 (bs, 2H), 2.07–2.25 (m, 3H), 2.56–2.61 (m, 2H), 4.21–4.24 (d, 1H, J = 10.5 Hz), 4.33–4.37 (d, 1H, J = 12.2 Hz), 4.54–4.60 (m, 1H), 4.82 (s, 1H, H-17), 5.01 (s, 1H, H-17), 5.08–5.13 (m, 1H), 5.39 (s, 2H), 5.93 (s, 1H), 5.98–6.00 (d, 1H, J = 6.03 Hz), 6.79–6.83 (m, 1H), 7.19–7.21 (d, 2H, J = 8.7 Hz, Ar), 7.50–7.53 (d, 2H, J = 8.7 Hz, Ar), 7.94–8.05 (dd, 4H, J = 8.8, 8.8 Hz, Ar), 8.41 (s, 1H), 9.08 (s, 1H triazole-H); ESI-MS: m/z 691 (M^+ 1) observed for $C_{36}H_{40}N_3O_6$.

3-(2-(3-(4-((1-(4-acetylphenyl)-1H-1,2,3-triazol-4-yl)methoxy) phenyl)-6a,10b-dimethyl-8-methylenedecahydro-1H-naphtho [2,1-d][1,3]dioxin-7-yl)ethylidene)-4-hydroxydihydrofuran-2 (3H)-one (3c). Yellow solid, yield 90%, mp 184–186°C; IR (KBr): 3279 (C–H), 3058 (Ar–H), 2922 (C–H), 2112 (C≡C), 1584 (C=N), 1466, 757 (C–N) cm^{-1}; ^{1}H NMR ($CDCl_3$, 300 MHz): δ 0.87 (s, 3H, H-20), 1.25 (s, 5H), 1.29–1.36 (m, 2H), 1.48 (s, 3H, H-18), 1.78–1.94 (m, 3H, AcO), 1.99–2.09 (m, 1H), 2.18 (s, 2H), 2.36–2.48 (m, 2H), 2.53–2.61 (m, 1H), 2.64 (s, 1H), 3.56–3.6 (d, 1H, J = 11.3 Hz), 3.64–3.68 (dd, 1H, J = 6.02, 5.52 Hz), 4.23–4.28 (m, 2H), 4.44–4.48 (m, 1H), 4.63 (s, 1H, H-17), 4.92 (s, 1H, H-17), 5.00–5.06 (d, 1H, J = 7.28 Hz), 5.32 (s, 2H), 5.73 (s, 1H), 6.95–6.98 (m, 1H), 7.00–7.03 (d, 2H, J = 9.03 Hz, Ar), 7.43–7.49 (m, 4H, Ar), 7.57–7.63 (m, 2H, Ar), 8.04 (s, 1H, triazole-H); ESI-MS: m/z 654 (M^+ 1) observed for $C_{38}H_{43}N_3O_7$.

3-(2-(3-(4-((1-(3-bromo-4-methylphenyl)-1H-1,2,3-triazol-4-yl)methoxy)phenyl)-6a,10b-dimethyl-8-methylenedecahydro-1H-naphtho[2,1-d][1,3]dioxin-7-yl)ethylidene)-4-hydroxydihydro furan-2(3H)-one (3d). Yellow solid, yield 91%, mp 176–177°C; IR (KBr): 3279 (C–H), 3058 (Ar–H), 2922 (C–H), 2112 (C≡C), 1584 (C=N), 1466, 757 (C–N) cm^{-1}; ^{1}H NMR ($CDCl_3$, 300 MHz): δ 0.86 (s, 3H, H-20), 1.28–1.50 (m, 4H), 1.53 (s, 3H, H-18), 1.71–1.80 (bs, 2H), 1.90–2.09 (bs, 2H), 2.07–2.25 (m, 3H), 2.56–2.61 (m, 2H), 4.21–4.24 (d, 1H, J = 10.5 Hz), 4.33–4.37 (d, 1H, J = 12.24 Hz), 4.54–4.60 (m, 1H), 4.82 (s, 1H), 5.01 (s, 1H), 5.08–5.13 (m, 1H), 5.39 (s, 2H), 5.93 (s, 1H), 5.98–6.00 (d, 1H, J = 6.03 Hz), 6.79–6.83 (m, 1H), 7.19–7.21 (d, 2H, J = 8.7 Hz, Ar), 7.50–7.53 (d, 2H, J = 8.7 Hz, Ar), 7.94–8.05 (dd, 4H, J = 8.8, 8.8 Hz, Ar), 8.41 (s, 1H), 9.08 (s, 1H); ESI-MS: m/z 705 (M^+ 1) observed for $C_{37}H_{42}BrN_3O_6$.

3-(2-(3-(4-((1-(2-chlorophenyl)-1H-1,2,3-triazol-4-yl)methoxy) phenyl)-6a,10b-dimethyl-8-methylenedecahydro-1H-naphtho [2,1-d][1,3]dioxin-7-yl)ethylidene)-4-hydroxydihydrofuran-2(3H)-one (3e). Yellow solid, yield 92%, mp 92°C; IR (KBr): 3279 (C–H), 3058 (Ar–H), 2922 (C–H), 2112 (C≡C), 1584 (C=N), 1466, 757 (C–N) cm^{-1}; ^{1}H NMR ($CDCl_3$, 300 MHz): δ 0.86 (s, 3H, H-20), 1.23–1.33 (m, 4H), 1.48 (s, 3H, H-18), 1.75–1.92 (m, 3H), 1.97–2.09 (m, 1H), 2.18 (s, 1H), 2.35–2.47 (m, 2H), 2.51–2.61 (m, 1H), 2.63 (s, 1H), 3.55–3.59 (d, 1H, J = 12.5 Hz), 3.63–3.69 (dd, 1H, J = 5.52, 5.52 Hz), 4.23–4.27 (m, 2H), 4.43–4.48 (m, 1H), 4.62 (s, 1H, H-17), 4.91 (s, 1H, H-17), 5.04–3.05 (d, 1H, J = 6.8 Hz), 5.32 (s, 2H), 5.73 (s, 1H), 6.94–6.98 (m, 1H), 7.01–7.03 (d, 2H, J = 9.03 Hz, Ar), 7.43–7.49 (m, 4H, Ar), 7.57–7.64 (m, 2H); ESI-MS: m/z 646 (M^+ 1) observed for $C_{36}H_{40}ClN_3O_6$.

3-(2-(3-(4-((1-(4-chlorophenyl)-1H-1,2,3-triazol-4-yl)methoxy) phenyl)-6a,10b-dimethyl-8-methylenedecahydro-1H-naphtho[2,1-d][1,3]dioxin-7-yl)ethylidene)-4-hydroxydihydrofuran-2(3H)-one (3f). Yellow solid, yield 85%, mp 200–202°C; IR (KBr): 3279 (C–H), 3058 (Ar–H), 2922 (C–H), 2112 (C≡C), 1584 (C=N), 1466, 757 (C–N) cm^{-1}; ^{1}H NMR ($CDCl_3$, 300 MHz): δ 0.87 (s, 3H, H-20), 1.25–1.30 (m, 4H), 1.48 (s, 3H, H-18), 1.56–1.66 (bs, 2H), 1.70–1.92 (m, 3H), 1.99–2.05 (m, 2H), 2.38–2.49 (m, 2H), 2.53–2.61 (m, 2H), 3.56–3.59 (d, 1H, J = 11.8 Hz), 3.64–3.69 (dd, 1H, J = 5.02, 5.02 Hz), 4.23–4.28 (m, 2H), 4.45–4.49 (m, 1H), 4.62 (s, 1H, H-17), 4.92 (s, 1H, H-17), 5.03–5.07 (m, 1H), 5.30 (s, 2H), 5.73 (s, 1H), 6.95–7.01 (m, 2H), 7.31–7.33 (d, 1H, J = 8.53 Hz, Ar), 7.43–7.45 (d, 1H, J = 9.03 Hz, Ar), 7.49–7.51 (d, 1H, J = 9.03 Hz, Ar), 7.67–6.69 (d, 2H, J = 9.03 Hz, Ar), 8.01 (s, 1H, triazole-H); ESI-MS: m/z 646 (M^+ 1) observed for $C_{36}H_{40}ClN_3O_6$.

3-(2-(6a,10b-dimethyl-8-methylene-3-(4-((1-(4-nitrobenzyl)-1H-1,2,3-triazol-4-yl)methoxy)phenyl)decahydro-1H-naphtho[2, 1-d][1,3]dioxin-7-yl)ethylidene)-4-hydroxydihydrofuran-2(3H)-one (3g). Yellow solid, yield 86%, mp 110–112°C; IR (KBr): 3279 (C–H), 3058 (Ar–H), 2922 (C–H), 2112 (C≡C), 1584 (C=N), 1466, 757 (C–N) cm^{-1}; ^{1}H NMR

($CDCl_3$, 300 MHz): δ 1.10 (s, 3H, H-20), 1.19–1.26 (m, 3H), 1.36–1.42 (m, 1H), 1.45 (s, 2H), 1.46 (s, 3H, H-18), 1.59 (s, 3H), 1.66 (s, 1H), 1.72–1.85 (m, 3H), 2.05–2.12 (m, 2H), 2.38–2.42 (d, 1H, J = 16.1 Hz), 2.56–2.68 (m, 1H), 3.01–3.08 (m, 1H), 3.22–3.29 (dd, 1H, J = 6.5, 6.78 Hz), 3.57–3.66 (m, 2H), 4.23–4.323 (m, 2H), 5.05–5.10 (t, 1H, J = 10.3 Hz), 5.24 (s, 1H), 5.63 (s, 1H), 5.70–7.71 (d, 1H, J = 5.5 Hz), 6.93 (s, 1H), 6.95 (s, 1H), 7.36–7.38 (d, 2H, J = 9.04 Hz, Ar), 7.40–7.43 (d, 2H, J = 8.8 Hz, Ar), 7.56 (s, 1H), 8.22 (s, 1H), 8.240 (s, 1H, triazole-H); ESI-MS: m/z 671 (M^+ 1) observed for $C_{37}H_{42}N_4O_8$.

3-(2-(3-(4-((1-benzyl-1H-1,2,3-triazol-4-yl)methoxy)phenyl)-6a,10b-dimethyl-8-methylenedecahydro-1H-naphtho[2,1-d][1,3]dioxin-7-yl)ethylidene)-4-hydroxydihydrofuran-2(3H)-one (3h). Yellow solid, yield 89%, mp 159–160°C; IR (KBr): 3279 (C–H), 3058 (Ar–H), 2922 (C–H), 2112 (C≡C), 1584 (C=N), 1466, 757 (C–N) cm^{-1}; ^1H NMR ($CDCl_3$, 300 MHz): δ 1.01 (s, 3H, H-20), 1.17–1.32 (m, 4H), 1.46 (s, 3H, H-18), 1.58 (s, 2H), 1.66 (s, 2H), 1.73–1.84 (m, 3H), 2.05–2.16 (m, 2H), 2.31–2.43 (m, 1H), 2.56–2.66 (m, 1H), 3.01–3.08 (m, 1H), 3.22–3.29 (dd, 1H, J = 6.5, 6.5 Hz), 3.56–3.65 (m, 2H), 4.23–4.31 (m, 2H), 4.45–4.51 (m, 1H), 5.05–5.10 (m, 1H), 5.18 (s, 1H), 5.52 (s, 1H), 5.69–5.70 (d, 1H, J = 5.02 Hz), 6.82–6.86 (m, 1H), 6.93–6.95 (d, 2H, J = 9.0 Hz), 7.27–7.28 (d, 1H, J = 2.8 Hz), 7.35–7.38 (m, 2H), 7.39–7.40 (d, 1H, J = 1.5 Hz, Ar), 7.41–7.42 (d, 2H, J = 1.76 Hz, Ar), 7.50 (s, 2H); ESI-MS: m/z 626 (M^+ 1) observed for $C_{37}H_{43}N_3O_6$.

3-(2-(6a,10b-dimethyl-8-methylene-3-(4-((1-phenethyl-1H-1,2,3-triazol-4-yl)methoxy)phenyl)decahydro-1H-naphtho[2,1-d][1,3]dioxin-7-yl)ethylidene)-4-hydroxydihydrofuran-2(3H)-one (3i). Yellow solid, yield 90%, mp 94–96°C; IR (KBr): 3279 (C–H), 3058 (Ar–H), 2922 (C–H), 2112 (C≡C), 1584 (C=N), 1466, 757 (C–N) cm^{-1}; ^1H NMR ($CDCl_3$, 300 MHz): δ 0.87 (s, 3H, H-20), 1.211–1.31 (m, 4H), 1.48 (s, 4H), 1.57–1.67 (m, 3H), 1.80–1.92 (m, 3H), 1.99–2.05 (m, 2H), 2.41–2.48 (m, 2H), 2.56–2.61 (m, 2H), 3.56–3.59 (d, 1H, J = 11.8 Hz), 3.64–3.66 (dd, 1H, J = 5.02, 5.02 Hz), 4.23–4.29 (m, 2H), 4.45–4.49 (m, 1H), 4.62 (s, 1H, H-17), 4.92 (s, 1H, H-17), 5.04–5.06 (d, 1H, J = 6.5 Hz), 5.30 (s, 2H), 5.73 (s, 1H), 6.96–7.01 (m, 3H), 7.43–7.45 (d, 2H, J = 9.0 Hz, Ar), 7.49 (s, 1H), 7.52 (s, 2H), 7.67–7.7 (d, 2H, J = 9.0 Hz, Ar), 8.01 (s, 1H, triazole-H); ESI-MS: m/z 640 (M^+ 1) observed for $C_{38}H_{45}N_3O_6$.

3-(2-(6a,10b-dimethyl-8-methylene-3-(4-((1-octyl-1H-1,2,3-triazol-4-yl)methoxy)phenyl)decahydro-1H-naphtho[2,1-d][1,3]dioxin-7-yl)ethylidene)-4-hydroxydihydrofuran-2(3H)-one (3j). Yellow solid, yield 83%, mp 78–80°C; IR (KBr): 3279 (C–H), 3058 (Ar–H), 2922 (C–H), 2112 (C≡C), 1584 (C=N), 1466, 757 (C–N) cm^{-1}; ^1H NMR ($CDCl_3$, 300 MHz): δ 0.85 (m, 8H), 1.25–1.31 (m, 14H), 1.48 (s, 3H), 1.76–1.83 (m, 1H), 1.86–1.91 (m, 4H), 2.40–2.47 (m, 2H), 2.55–2.63 (m, 2H), 3.55–3.58 (dd, 1H, J = 1.3, 1.5 Hz), 3.63–3.68 (m, 1H), 4.23 (s, 1H), 4.25–4.28 (dd, 1H, J = 2.3, 2.3 Hz), 4.31–4.34 (t, 3H), 4.44–4.48 (m, 1H), 4.62 (s, 1H), 4.91 (s, 1H), 5.04–5.06 (d, 1H, J = 6.53 Hz), 5.21 (s, 2H), 5.7 (s, 1H), 6.90 (s, 1H), 6.98–7.00 (m, 1H), 7.41 (s, 1H), 7.42 (s, 1H), 7.56 (s, 1H); ESI-MS: m/z 648 (M^+ 1) observed for $C_{38}H_{53}N_3O_6$.

3-(2-(6a,10b-dimethyl-8-methylene-3-(4-((1-pentyl-1H-1,2,3-triazol-4-yl)methoxy)phenyl)decahydro-1H-naphtho[2,1-d][1,3]dioxin-7-yl)ethylidene)-4-hydroxydihydrofuran-2(3H)-one (3 k). Yellow solid, yield 83%, mp 81°C; IR (KBr): 3279 (C–H), 3058 (Ar–H), 2922 (C–H), 2112 (C≡C), 1584 (C=N), 1466, 757 (C–N) cm^{-1}; ^1H NMR ($CDCl_3$, 300 MHz): δ 0.88 (m, 3H, H-20), 1.24–1.26 (m, 6H), 1.3–1.32 (s, 3H, H-18), 1.37 (s, 1H), 1.66 (s, 1H), 1.8–1.83 (m, 2H), 1.86–1.92 (m, 3H), 2.41–2.45 (dd, 1H, J = 3.36, 3.012 Hz), 2.49–2.50 (m, 2H), 2.55–2.61 (m, 3H), 3.56–3.61 (m, 1H), 3.64–3.69 (m, 2H), 4.23–4.25 (m, 1H), 4.26–4.302 (m, 2H), 4.44–4.49 (m, 2H), 4.62 (s, 1H, H-17), 4.92 (s, 1H, H-17), 5.73 (s, 2H), 6.95–6.96 (d, 2H, J = 2.3 Hz), 6.97–6.98 (m, 2H), 7.42–7.43 (d, 2H, J = 2.3 Hz, Ar), 7.44–7.45 (d, 1H, J = 2.0 Hz, Ar); ESI-MS: m/z 606 (M^+ 1) observed for $C_{35}H_{47}N_3O_6$.

Pharmacological screening. ***Biology in vitro assays.*** Seven different human cancer cell lines were used under study MCF7 (breast), MDA-MB-231 (breast), COLO205 (colorectal), HepG2 (hepato), K562 (myelogenous leukemia), HeLa (cervical), and HEK293 (normal human kidney embryonic). The cells lines were obtained from the National Centre for Cell Sciences, Pune, India, and were cultured at a seeding density of 0.2×10^6 in Dulbecco's modified Eagle's medium/Roswell Park Memorial Institute (RPMI), medium supplemented with 10% fetal bovine serum, 100-U/mL penicillin, and 100-μg/mL streptomycin, respectively, and maintained in a humidified atmosphere with 5% CO_2 at 37°C. The samples were dissolved in DMSO (not exceeding the final concentration of 0.01%) and further diluted in cell culture medium. The anti-proliferative response of extract was assessed by MTT assay [23]. Cells (~5000) were plated in 200-μL growth medium in the presence or absence of the test samples under study (50-μ*M* concentration); negative control blank (DMSO) and positive control (doxorubicin 10 n*M*) were used for comparison, which were added in 96 well culture plates and incubated for 24 h with a 90% humidified atmosphere and 5% CO_2. Then the culture plates were centrifuged at 2000 rpm for 10 min at room temperature; 100 μL of supernatant was discarded, and 20 μL of MTT (5 mg/mL in phosphate-buffered saline) was added to each well, incubated for 4 h at 37°C. Add 100 μL of DMSO in each well at 37°C for 5 min. The purple formazan crystals were dissolved, and immediately, read absorbance at 570 nm was measured using Spectra Max plus 384 UV-visible plate reader (Molecular Devices, Sunnyvale, CA, USA). IC_{50} values were determined by probit analysis software package of MS-excel [% cell viability (from

control) versus concentration]. The IC_{50}, that is, the concentration (IC_{50} 5–50 μM), of the test samples required to inhibit cell growth by 50% was determined.

Virtual screening by molecular docking studies. Initially, the protein preparation protocol was used to perform tasks such as inserting missing atoms in incomplete residues, deleting alternate conformations, removing water, standardizing names of the atoms, and valency and hydrogen bonding of the ligands, and target protein was subsequently satisfied. Polar hydrogen atoms were added to the protein target to achieve the correct ionisation and tautomeric states of amino acid residues such as His, Asp, Ser, and Glu. The molecular docking studies were performed to generate the active binding poses of candidate compounds in the active site of the receptor by using Autodock VINA software (Prentice, WI, USA). Binding pose with the lowest docked energy belonging to the top-ranked cluster was selected as the final model for post-docking analysis with PyMOL and Discovery Studio v3.5. The geometry cleaning of all 12 compounds was performed through ChemBioDraw-Ultra-v12.0 (Cambridge Soft, UK). The 3D structures were subjected to energy minimization. Energy minimized by using molecular mechanics-2 force field until the root mean square gradient value became smaller than 0.100 kcal/mol-1/Å. Re-optimization was carried out by Molecular Orbital Package method until the root mean square gradient attained a value smaller than 0.0001 kcal/mol-1/Å. The 3D chemical structure of known drug capsaicin (CID_1548943) was retrieved from PubChem (NCBI, USA).

Acknowledgments. The authors thank Director, CSIR-CIMAP, Lucknow, India, and Scientist Incharge, CSIR-CIMAP-RC, Hyderabad, India for their constant encouragement and support. Author Yakaiah thanks CSIR-New Delhi for granting Senior Research Fellowship. Manjulatha K thanks DST WOSA for financial assistance and Feroz Khan aknowledge financial support through SERB, Department of Science & Technology, New Delhi, India.

REFERENCES AND NOTES

[1] Ma, X. C.; Zhang, B. J.; Deng, S.; Huang, S. S.; Liu, K. X.; Jia, J. M. Chin ChemLett 2009, 20, 317.

[2] Shen, Y. H.; Li, R. T.; Xiao, W. L.; Xu, G.; Lin, Z. W.; Zhao, Q. S.; Sun, H. D. J. Nat Prod 2006, 69, 319.

[3] Saraswat, B.; Visen, P. K. S.; Patnaik, G. K.; Dhawan, B. N. Fitoterapia 1995, 66, 415.

[4] Gupta, S.; Choudhry, M. A.; Yadava, J. N. S.; Srivastava, V.; Tandon, J. S. Int J Crude Drug Res 1990, 28, 273.

[5] Deng, W. L. Drugs Future 1990, 15, 809.

[6] Madav, S.; Tanda, S. K.; Lal, J.; Tripathi, H. C. Fitoterapia 1996, 67, 452.

[7] Kumar, R. A.; Sridevi, K.; Kumar, N. V.; Nanduri, S.; Rajagopal, S. J Ethnopharm 2004, 92.

[8] Calabrese, C.; Berman, S. H.; Babish, J. G.; Ma, X.; Shinto, L.; Dorr, M.; Wells, K.; Wenner, C. A.; Standish, L. J. Phytother Res 2000, 14, 333.

[9] Sirinivasa, R. J.; Genevieve, S. S.; Charile, M.; Ahmad, S. H.; Nordin, H. L.; Mohammad, S. S.; Malcolm, F. S.; Hohnson, S. Phytochemistry 2007, 68.

[10] Das, B.; Chowdhury, C.; Kumar, D.; Sen, R.; Roy, R.; Das, P.; Chatterjee, M. Bioorg Med Chem Lett 2010, 20, 6947.

[11] Dai, G. F.; Xu, H. W.; Wang, J. F.; Liu, F. W.; Liu, H. M. BioorgMed Chem Lett 2006, 16, 2710.

[12] Srinivas, N.; Vijay, K. N.; Siva, S. R. T.; Sridevi, K.; Mahesh, K. P.; Sriram, R.; Rajagopalan, R.; Venkateswarlu, A. Bioorg Med Chem Lett 2004, 14.

[13] Li, J.; Huang, W.; Zhang, H.; Wang, X.; Zhou, H. Bioorg Med Chem Lett 2007, 17, 6891.

[14] Sheremet, E. A.; Tomanov, R. I.; Trukhin, E. V.; Berestovitskaya, V. M. Russ J Org Chem 2004, 40, 594.

[15] Allais, A.; Meier, J. (Roussele Uclaf) (1969) Novel quinolines. DE Patent 1815467.

[16] Diana, G. D.; Nitz, T. J.; (Sterling Winthrop). EP Patent 0566199 (1993).

[17] Julino, M.; Stevens, M. F. G. J Chem Soc Perkin Trans 1998, 1, 1677.

[18] Syed, S.; Mohammad, M. A.; Naveen, M.; Chaithanya, M.; Vanaja, G.; Arunasree, M. K.; Reddanna, P.; Alam, M. S. Eur J Med Chem 2012, 49, 324.

[19] Semenova, S. B.; Vassilieva, I. O.; Fomina, A. F.; Runov, A. L.; Negulyaev, Y. A. Am J Physiol Cell Physiol 2009, 296, 1098.

[20] Sung, B.; Prasad, S.; Ravindran, J.; Yadav, V. R.; Aggarwal, B. B. Free Radic Biol Med 2012, 53, 1977.

[21] Vercelli, C.; Barbero, R.; Cuniberti, B.; Odore, R.; Re, G. Vet Comp Oncol 2013, 19, 9999.

[22] Egan, W. J.; Merz, K. M.; Baldwin, J. J. J Med Chem 2000, 43, 3867.

[23] Mosmann, T. J Immunol Meth 1983, 65, 55.